Hydromechanical modelling of shaft sealing for CO_2 storage

A.C. Dieudonne[a,b,*], B. Cerfontaine[a], F. Collin[a], R. Charlier[a]

[a] University of Liege, ArGEnCo Department, ArGEnCo Department, Chemin des Chevreuils 1, 4000 Liege, Belgium

Email addresses: ac.dieudonne@ulg.ac.be, b.cerfontaine@ulg.ac.be, f.collin@ulg.ac.be, robert.charlier@ulg.ac.be

[b] F.R.I.A., Fonds de la Recherche Scientifique – FNRS, Rue d'Egmont 5, 1000 Brussels, Belgium

* Correspondence to: University of Liege, ArGEnCo Department, Chemin des Chevreuils 1, 4000 Liege, Belgium

Phone number: +32 (0)4 366 20 31

Email address: ac.dieudonne@ulg.ac.be

Abstract

The geological sequestration of CO_2 in abandoned coal mines is a promising option to mitigate climate changes while providing sustainable use of the underground cavities. In order to certify the efficiency of the storage, it is essential to understand the behaviour of the shaft sealing system. The paper presents a numerical analysis of CO_2 transfer mechanisms through a mine shaft and its sealing system. Different mechanisms for CO_2 leakage are considered, namely multiphase flow through the different materials and flow along the interfaces between the lining and the host rock. The study focuses on the abandoned coal mine of Anderlues, Belgium, which was used for seasonal storage of natural gas. A two-dimensional hydromechanical modelling of the storage site is performed and CO_2 injection into the coal mine is simulated. Model predictions for a period of 500 years are presented and discussed with attention. The role and influence of the interface between the host rock and the concrete lining are examined. In addition the impact of some uncertain model parameters on the overall performance of the sealing system is analysed through a sensitivity analysis.

Keywords: CO_2 storage; abandoned coal mines; gas migration; numerical modelling; interface behaviour

1. Introduction

Carbon capture and storage has a considerable potential for mitigating climate changes through the reduction of greenhouse gas emissions. The technique consists in trapping, transporting and sequestrating carbon dioxide (CO_2) into deep geological formations. Appropriate reservoirs for the storage of CO_2 include depleted oil and gas reservoirs, deep saline aquifers and unminable coal seams. In the latter case, adsorption of CO_2 onto the coal surface is the main trapping mechanism (White et al., 2005). Indeed, coal is characterized by a very high internal surface area (ranging from 20 to 300 m^2/g) on which large quantities of CO_2 can be adsorbed (Gaucher et al., 2011). However injection of carbon dioxide into coal formations triggers complex coupled phenomena between the fluids and the coal formation. In particular CO_2 adsorption onto the coal particles induces swelling and important permeability modifications of the porous medium (see for instance Gray, 1987; Seidle and Huitt, 1995; Connell, 2009; Chen et al., 2010, Espinoza et al., 2014). As a consequence, the injection rate of carbon dioxide into the formation can decrease drastically and jeopardize the viability of the operations.

In order to avoid these problems, several studies have focused on the use of abandoned coal mines as potential reservoirs (Piessens and Dusar, 2004; van Tongeren and Dreesen, 2004; Kempka et al., 2006; Romanov et al., 2009; Lutynski, 2010; Jalili et al., 2011). Injection of CO_2 into abandoned coal mines would indeed benefit from the important storage capacity of the host rock (still rich in coal and clay minerals) while the fractured zone around the cavities would enhance injection. Due to their abundance and their location generally close to important point sources, abandoned coal mines could represent interesting opportunities for the sequestration of carbon dioxide. In addition, injection of CO_2 into these mines could benefit from the co-production of methane (see for instance Pini et al., 2009).

Since 1961 at least three abandoned coal mines have been used for the seasonal storage of natural gas. In Belgium, the coal mines of Anderlues and Peronnes were exploited between

1980 and 2000 by Fluxys (Houtrelle, 1999; Piessens and Dusar, 2004; van Tongeren and Dreesen, 2004). In the United States, natural gas was stored in the coal mine of Leyden, Colorado, since the sixties. The last storage site however closed in 2001 because of important gas leakage through the wells (EPA, 1998; Schultz, 1998; BGS, 1998).

From these experiences, it appears that not only the efficiency of the storage relies on the geological configuration, but the presence of manmade discontinuities, such as shafts, should be considered. Safety assessment of CO_2 storage requires therefore a precise understanding of the transfer mechanisms through the shaft and its sealing system. Numerical modelling provides an important tool for such analysis which should be performed over large scale and long time periods. In the last decade, the injection of carbon dioxide into deep saline aquifers and depleted hydrocarbon fields have been studied by various authors (see for instance Rutqvist and Tsang, 2002; Vilarrasa et al., 2010; Alonso et al., 2012; Laloui and Li, 2015 for saline aquifers, Durucan, 2009; Vidal-Gilbert et al., 2009 for hydrocarbon fields). The questions of CO_2 leakage along wellbores and wellbore integrity have also been addressed in the context of deep sequestration of supercritical CO_2 (Celia et al., 2005; Watson et al., 2009; Sy et al., 2012). Nonetheless the efficiency of the sealing systems of mine shafts in the context of shallow CO_2 sequestration has been disregarded.

The paper presents a numerical analysis of CO_2 transfer mechanisms through and around a shaft sealing system. The abandoned coal mine of Anderlues, which was used for seasonal storage of natural gas, provides the context of the study. The finite element code LAGAMINE (Charlier et al., 2001; Collin et al., 2002) has been used in this work to study the problem from a numerical point of view. The paper is organized as follows: the storage site and its geological context are described first, followed by a description of the hydromechanical formulation used to carry out the analysis. For the sake of clarity, a first modelling assuming perfect contact between the materials is performed. The features of the numerical analysis are presented and the results of

the simulations are discussed. The impact of some uncertain model parameters on the overall performance of the sealing system is analysed through a sensitivity analysis. Finally, the role and influence of the interface between the host rock and the concrete lining are assessed through a series of numerical simulations using interface finite elements.

2. Anderlues coal mine and gas storage facility

2.1. Geological and hydrogeological setting

The coal mine of Anderlues is located in South-Western Belgium. From a geological point of view, the region corresponds to the coal Basin of Mons. These rocks date from the Upper Carboniferous Westphalian (313 – 304 Ma), a geological stage during which the region of Mons was subjected to an important compressive tectonic setting (Sudetian phase of the Variscan Orogeny). The Westphalian formations are characterized by a cyclicity which is typical from paralic deposits. Alternating sequences of shale, deposited during subsidence episodes, and of plant debris, which progressively turned into coal in the absence of oxygen, are observed (Delmer *et al*., 2001; Boulvain and Pingot, 2012).

Deposits from the Mesozoic and Cenozoic eras form the overburden. They are characterized by lacustral and alluvial continental facies (gravels, sands, ferruginous sandstones and clays), and later by marine facies (marls, clays and chalks). Their average thickness is about 50 meters.

The Westphalian rocks are composed of 60% of shale, 37% of sandstone and 3% of coal (Ghiste, 1990). The shale is made of alumina silicate Al_2SiO_5 which contains less water than clays. In contact with water, the shale tends to rehydrate and swell, hence turning into clay. This clay induces clogging of the porous space and therefore decreases the hydraulic conductivity of the rock. This low-permeability interface limits the infiltration of meteoric water into the shale rock which is consequently unsaturated in Anderlues.

2.2. Coal mining and natural gas storage

Coal exploitation in Anderlues occurred between 1857 and 1969. During this period, 25 Mton of coal were extracted from the soil, which corresponds to only 3,5% of the total coal volume in the ore. The 96,5% remaining are considered difficult to exploit because of their spatial scattering (Vandeloise, 1969).

From 1966, different tests were performed in order to study the possibility to capture firedamp (mostly composed of methane) from the mine. Indeed, the coalfields from the Mons Basin are known to hold large amounts of gas, as during mining important volumes of firedamp adsorbed on the coal were released. Vandeloise (1969) estimated the firedamp reserves to about 5 to 6 st-Gm^3. In 1978, only 70 Mm^3 had been captured.

The large amount of naturally adsorbed methane demonstrates that gas can be safely retained for thousands of years and that the coalfields from the Mons Basin could therefore be used as reservoirs. In 1978, Distrigaz (currently Fluxys) decided to use the former coal mine as a reservoir for seasonal storage of natural gas. Natural gas was stored under low pressure conditions (under 0.35 MPa) between 600 and 1100 meters depth. 90% of the gas stored was adsorbed on the coal particles surface. Nine piezometers were drilled in the overburden to check the efficiency and safety of the gas storage. Piezometer levels did not exhibit any change due to injection or production of gas. Although no leakage was observed, the gas storage facility closed in 2000 because of the need for costly maintenance work at the shafts (Piessens and Dusar, 2004).

Fig. 1 presents the shaft sealing system that was used in Anderlues. The geometry is the one of the shaft n°6. It is composed to two concrete slabs for sealing and strength reasons. In between a bentonite plug is used as a secondary seal.

In 2008, the Policy Support System for Carbon Capture and Storage (PSS-CCS) project analysed the opportunities of implementing carbon capture and storage in the Belgian context (Piessens et al. 2008). Among the various options, coal mines at relatively shallow depths were considered for CO_2 sequestration under gas phase. Although supercritical storage of CO_2 would be more ideal from an economical point of view, coal mines have ideal location close to important point sources and the cost for CO_2 transport would therefore be reduced. In addition, CO2 storage in abandoned coal mines is believed to more easily benefit from public acceptance (Piessens and Dusar 2004).

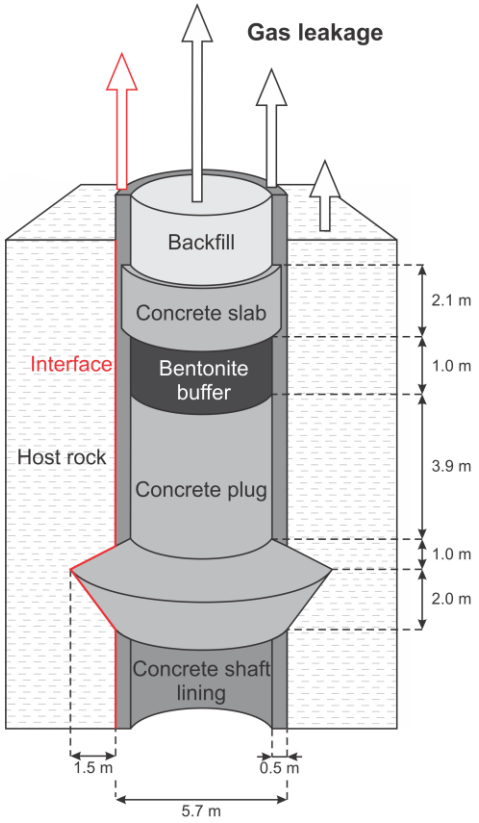

Fig. 1: Layout of the sealing system used for the shaft n°6 of Anderlues coal mine

3. Coupled HM formulation

In the present study, injection of CO_2 at relatively shallow depths is considered. Under the considered pressure and temperature conditions, CO_2 is a gas and the hydromechanical formulation proposed in Collin et al. (2002) is considered. The theoretical framework is

formulated using a multiphase (solid, liquid and gas), multispecies approach (mineral, water and CO_2). The liquid phase is assumed to be composed of both liquid water and dissolved CO_2, while the gas phase contains dry CO_2 and water vapour. The presence of air in the porous media is thus neglected.

The theoretical framework is composed of three balance equations, namely the balance of momentum (or stress equilibrium) equation and the mass balance equations for water and CO_2. The stress equilibrium equation is expressed as:

$$div(\sigma) + b = 0$$

(1)

where σ is the total (Cauchy) stress tensor and b is the body force vector.

The mass balance equations for water and CO_2 are given by:

$$\underbrace{div\left(\underline{f_w}\right) + \frac{\partial}{\partial t}\left(\rho_w \phi S_{r,w}\right)}_{Liquid\ water} + \underbrace{div\left(\underline{f_v}\right) + \frac{\partial}{\partial t}\left(\rho_v \phi\left(1 - S_{r,w}\right)\right)}_{Water\ vapour} - Q_w = 0$$

(2)

$$\underbrace{div\left(\underline{f}_{CO_2}\right) + \frac{\partial}{\partial t}\left(\rho_{COo_2}\phi\left(1 - S_{r,w}\right)\right)}_{Dry\ CO_2 in\ gas\ phase} + \underbrace{div\left(\underline{f}_{CO_2-d}\right) + \frac{\partial}{\partial t}\left(\rho_{CO_2-d}\phi S_{r,w}\right)}_{Dissolved\ CO_2 in\ water} - Q_{CO_2} = 0$$

(3)

where ρ_v, ρ_{CO2} and $\rho_{CO2\text{-}d}$ are respectively water vapour, CO_2 and dissolved CO_2 bulk densities, $\underline{f_w}$, $\underline{f_v}$, $\underline{f}_{CO_2}$ and $\underline{f}_{CO_2-d}$ are the total mass flow respectively for liquid water, water vapour, CO_2 and dissolved CO_2. Finally, Q_w and Q_{CO_2} are volumes sources of water and carbon dioxide.

A two-phase flow model is considered for the description of the fluid transport processes. Mass flows take into account the advection of each phase and the diffusion of the components within each phase:

$$\underline{f_w} = \rho_w \underline{q_l}$$

(4)

$$f_v = \rho_v \underline{q_g} + \underline{i_v}$$

(5)

$$\underline{f_{CO_2}} = \rho_{CO_2} \underline{q_g} + \underline{i_{CO_2}}$$

(6)

$$f_{CO_2-d} = \rho_{CO_2-d} \underline{q_l} + \underline{i_{CO_2-d}}$$

(7)

where $\underline{q_l}$ and $\underline{q_g}$ are respectively the advective fluxes of the liquid and the gaseous phases, and $\underline{i_v}$, $\underline{i_{CO_2}}$ and $\underline{i_{CO_2-d}}$ the diffusion fluxes respectively for the water vapour, the dry carbon dioxide and the dissolved carbon dioxide. Diffusion of water within the liquid phase is neglected due to relatively gas pressures involved in the problem (Corey et al., 2010).

The advection of each phase is described by the generalized Darcy's law for unsaturated media:

$$\underline{q_l} = -\frac{K_{int}\, k_{rw}}{\mu_w}\left(\underline{grad}(p_w) + g\, \rho_w \underline{grad}(y)\right)$$

(8)

$$\underline{q_g} = -\frac{K_{int}\, k_{rg}}{\mu_g}\left(\underline{grad}(p_g) + g\, \rho_g \underline{grad}(y)\right)$$

(9)

where K_{int} is the intrinsic permeability, k_{rw} and k_{rg} are the water and gas relative permeabilities, μ_w and μ_g are the water and gas dynamic viscosities and *y* is the vertical upward directed coordinate.

The diffusion of the components within each phase writes (Fick's law):

$$\underline{i_v} = -\phi\left(1 - S_{r,w}\right)\tau D_{v/CO_2} \rho_g \underline{grad}\left(\frac{\rho_v}{\rho_g}\right) = -\underline{i_{CO_2}}$$

(10)

$$\underline{i}_{CO_2-d} = -\phi S_{r,w} \tau D_{CO_2-d/w} \rho_w \underline{grad} \left(\frac{\rho_{CO_2-d}}{\rho_w} \right)$$

(11)

where D_{v/CO_2} and $D_{CO_2-d/w}$ are the diffusion coefficient respectively in the gaseous mixture dry carbon dioxide – water vapour and for the dissolved carbon dioxide in water, and τ is the tortuosity of the porous medium.

4. Features of the analysis

A two-dimensional axisymmetric analysis is performed considering the geometry shown in Fig. 2. The geometry of the problem is based on the mine shaft n°6 from the Anderlues coal mine and on the sealing system that was used by Fluxys for the storage of natural gas. The materials considered in the model are the host rock, the concrete shaft lining, plug and slab, the bentonite buffer and the backfill. The vertical extension of the model is 100 meters so that the upper boundary corresponds to the limit between the Palaeozoic and Mesozoic formations. The radial outer boundary is placed at a distance of 100 meters from the shaft axis. An investigation into the element size and type was conducted to ensure good spatial convergence of the results. The mesh is composed of 2222 eight-noded isoparametric quadrilateral elements with nine integration points.

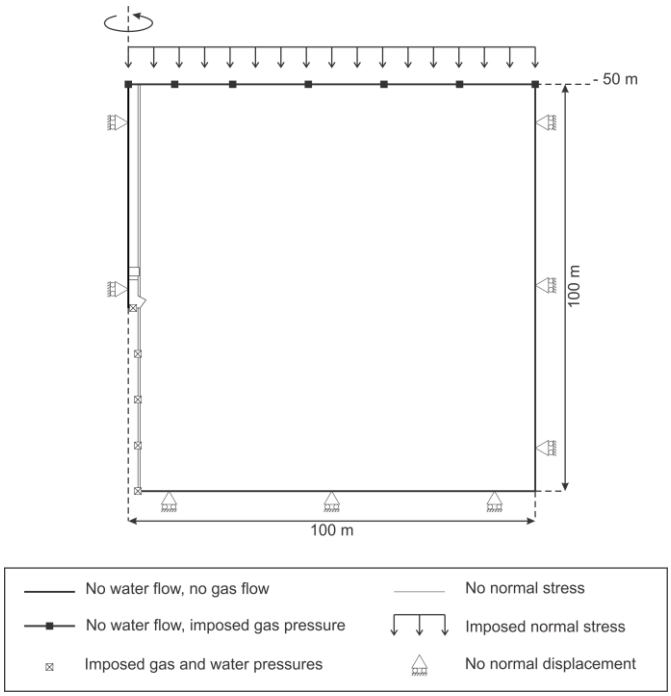

Fig. 2: Geometry and boundary conditions used for the hydromechanical analysis

The simulation consists in 4 different stages: (1) the shaft excavation, (2) the set-up of the concrete shaft lining and ventilation of the mine, (3) the set-up of the sealing system, and (4) the injection of CO_2 into the mine. Essentially, the first three stages are performed in order to establish the hydromechanical conditions in the different materials prior to CO_2 injection. During these stages, a constant and uniform gas pressure equal to atmospheric is assumed throughout the whole domain. Due to phasing of the modelling, only the shale elements are included in the mesh during the first stage. Elements from the shaft lining and the sealing system are respectively introduced during the second and third stages of the simulation.

The analysis starts simulating the shaft excavation within 50 days. The initial stress field in the shale is assumed isotropic. At the envisaged depths of the analysis, the influence of gravity may not be neglected and the initial stresses in the shale are induced by gravity loads arising from its own weight. The initial hydric state of the shale is not precisely known but unsaturated. An initial water pressure of -3,43 MPa, corresponding to a degree of saturation close to 90%, is

assumed. In addition, a sensitivity analysis is performed on the host rock initial degree of saturation in order to assess its influence on the global efficiency of the storage system. During the excavation stage, the water pressures at the shaft wall are progressively brought to a value of -30 MPa, corresponding to a relative humidity of 80%. This value was selected based on the average relative humidity in Belgium, ranging between 80% and 90%, and assuming a thermodynamic equilibrium between the cavity air and the geological formation (Gerard et al., 2008).

The second stage of the simulation corresponds to the set-up of the concrete shaft lining and to a ventilation phase of 50 years (coal mining). Then the sealing system is placed and water pressures are allowed to equilibrate for 50 days. As for the shale, the initial stress field in the concrete, bentonite and backfill elements is isotropic and gravity loads are considered. Initial water pressures in these elements are supposed to be in equilibrium with the shaft relative humidity of 80%. It is assumed that there is perfect contact between the different materials.

The last stage of the analysis consists in the injection of CO_2 into the mine. Gas pressures at the shaft wall and at the basis of the sealing system are increased at a rate of 0,25 MPa/year for 10 years and are then maintained constant. Water pressures at these boundaries are maintained constant and equal to -30 MPa as for the previous stages.

5. Material parameters

The problem under consideration consists of four different materials: the host shale rock, the concrete shaft lining and sealing systems, a bentonite buffer and a backfill. Each of these materials requires the definition of a full set of hydromechanical parameters.

5.1. Mechanical properties

Shaft excavation is likely to induce yielding of the host rock, hence producing an Excavated Damaged Zone (EDZ). Therefore the mechanical behaviour of the shale is modelled with an associated elastoplastic perfectly plastic law, defined by Drucker-Prager yield criterion. Parameters were determined from laboratory experiments carried out by Fluxys (1990), assuming isotropy (Ramos da Silva et al., 2008). The Biot coefficient, used in Bishop's definition of effective stress (Nuth and Laloui, 2007), is deduced from the shale porosity using Fabre and Gustkiewicz's exponential law (1997):

$$b = 1 - \exp(-a \tan\left(\frac{\pi}{2}\phi\right)) \quad (12)$$

where Φ is the porosity and a is an empirical coefficient depending on the rock type. Ramos da Silva et al. (2008) suggests a value of a equal to 5 in the case of shale, giving a value of Biot coefficient equal to 0,4. Such low values for Biot coefficient are found in low-porosity shale rocks (Cosenza et al., 2002; Bemer et al., 2004; Willeveau, 2005; Hou et al., 2010).

Under the considered stress conditions, concrete, bentonite and the backfill material exhibit an elastic behaviour and linear elastic laws are used as a first approximation. The values of the mechanical parameters correspond to materials that are studied for the geological disposal of radioactive wastes and were presented in Gerard et al. (2008). The mechanical parameters for the different materials are summarized in Table 1.

		Shale	Concrete	Bentonite	Backfill
E	Young's modulus (MPa)	3000	33000	150	38.5
ν	Poison's ratio (-)	0.3	0.16	0.3	0.2
c	Cohesion (MPa)	2.66	-	-	-
φ	Friction angle (°)	22.7	-	-	-
b	Biot's coefficient (-)	0.4	0.8	1	1

Table 1: Mechanical parameters for the different materials

5.2. Hydraulic properties

The water retention curve relates suction with degree of saturation. Van Genuchten model (Van Genuchten, 1980) is adopted to represent the water retention behaviour of the different materials. It writes:

$$S_{r,w} = \left[1 + \left(\frac{s}{P_r}\right)^n\right]^{-m}$$

(13)

where P_r is a parameter related to the air-entry pressure and n and m are van Genuchten's parameter.

Van Genuchten water relative permeability model is adopted for the different materials:

$$k_{rw} = \sqrt{S_{r,w}}\left(1 - \left(1 - S_{r,w}^{\frac{1}{m}}\right)^m\right)^2$$

(14)

The hydraulic parameters of the different materials are presented in Table 2. The parameters of the retention curve of the host rock were determined fitting experimental data obtained by Ramos da Silva et al. (2008) on Westphalian shale from the Beringen coal mine, located some 130 km North-East from Anderlues (Fig. 3). Parameters values from the literature are adopted for the hydraulic parameters of concrete, bentonite and the backfill material (Gerard et al., 2008).

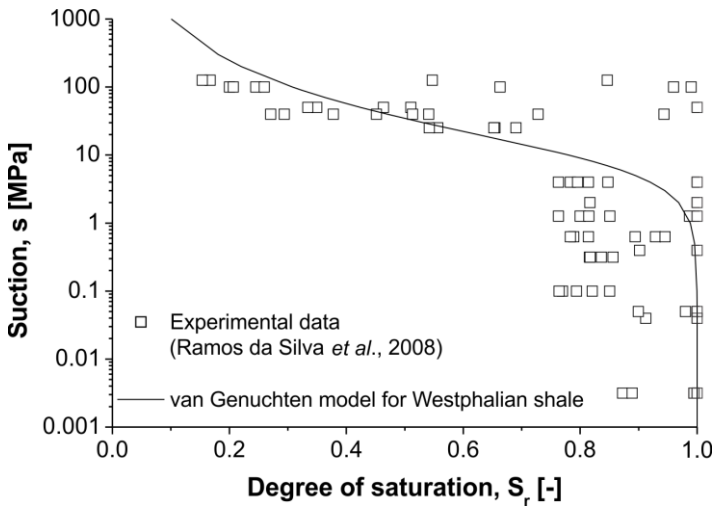

Fig. 3: Water retention curve of Beringen shale (data are from Ramos da Silva et al., 2008)

Gas relative permeability is modelled using the following cubic law (Pintado et al., 2002; Chen et al., 2012):

$$k_{rg} = \left(1 - S_{r,w}\right)^3 \quad (15)$$

		Shale	Concrete	Bentonite	Backfill
K_{int}	Intrinsic permeability (m²)	$2\ 10^{-19}$	$1\ 10^{-16}$	$8\ 10^{-21}$	$1\ 10^{-15}$
Φ	Porosity (-)	0.054	0.15	0.37	0.33
τ	Tortuosity (-)	0.25	0.25	0.0494	1
P_r	Van Genuchten parameter (MPa)	9.2	2	16	0.12
n	Van Genuchten parameter (-)	1.49	1.54	1.61	1.4203
m	Van Genuchten parameter (-)	0.33	0.35	0.38	0.30

Table 2: Hydraulic parameters for the different materials

6. Model results and analysis

6.1. Shaft excavation and ventilation (stages 1-3)

Fig. 4 presents the evolution of pore water pressure profiles in the shale during the shaft excavation. The values at the shaft wall correspond to the imposed boundary conditions. The water pressure drawdown causes water flows towards the shaft axis, hence creating a cone of depression. Owing for the weak permeability of the shale, the extension of the cone is limited after 50 days: important pore pressure changes are concentrated on the first 300 mm of the host rock. By the end of the excavation, the water saturation at the shaft wall has reached 53%. In addition, the shaft convergence is of the order of 5 mm, preserving the elastic character of the host rock.

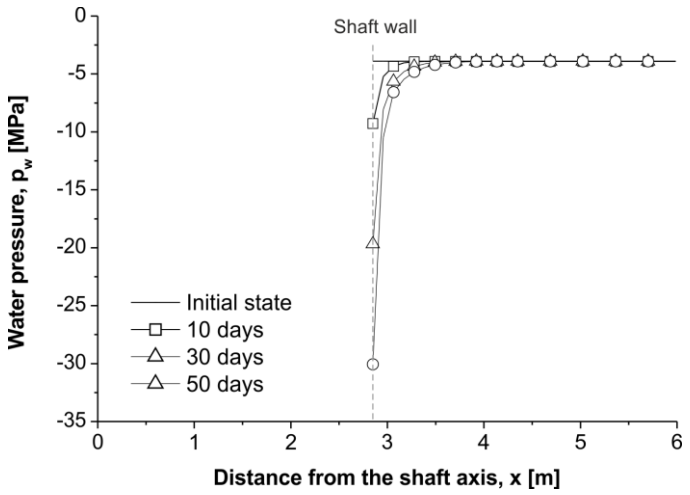

Fig. 4: Evolution of pore water pressure profiles in the shale during the shaft excavation

Fig. 5 presents the evolution of the water pressures profiles once the concrete shaft lining is set up. The water pressure in the shaft lining is initially in equilibrium with the shaft relative humidity. Competing effects from the low-suction imposed boundary condition and the host rock are observed. Indeed at the beginning of the stage, the difference in water pressures between the concrete lining and the host rock causes water flows from the shale towards the lining, hence resaturating the concrete. However after 3 years, the imposed relative humidity becomes progressively prominent and the concrete saturation tends to decrease, before reaching equilibrium.

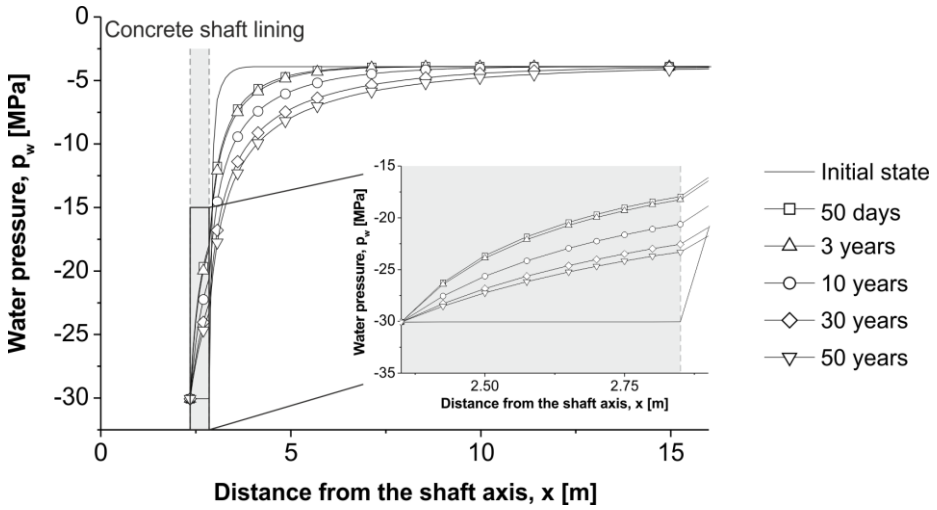

Fig.5: Evolution of pore water pressure profiles in the shale and the support during shaft ventilation

By the end of ventilation stage, water pressures in the shale are disturbed over a distance smaller than 10 meters. At the shaft wall, the water saturation of the shale is 60% while it was initially of 90%. Because of its retention properties, the concrete has a low water degree of saturation, which is about 25%. Finally, the important air entry pressure of bentonite gives a degree of saturation of about 60%.

6.2. CO_2 injection (stage 4)

Carbon dioxide injection into the coal mine is modelled increasing the gas pressures at the shaft wall and at the basis of the sealing system. Fig. 6 shows the distribution of gas pressures in the sealing system and the zone around the shaft. We observe that the increase in gas pressure is essentially localized in the concrete elements. The CO_2 indeed circulates preferentially in the porous medium that presents the smallest opposition. In weakly saturated porous media, gas flow occurs mainly through advection. Carbon dioxide transfer kinetics is therefore mainly driven by the medium permeability. Given the weak water saturation of concrete (which is around 23% where gas and water pressures are imposed) and its higher intrinsic permeability,

the gas flow occurs essentially through the concrete elements of the supporting and sealing systems. Conversely, the bentonite buffer acts as a quasi-impermeable frontier.

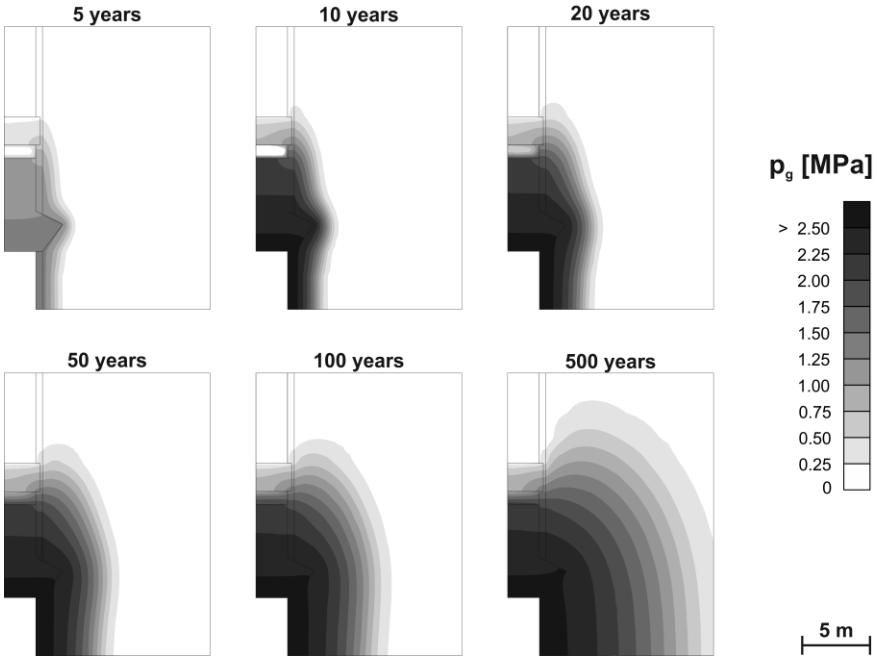

Fig. 6: Evolution of gas pressures in the different materials during CO_2 storage in the coal mine

Table 3 gives the distribution of the CO_2 masses rejected to the atmosphere through each material. We observe that because of its high permeability, the backfill drains almost all CO_2 fluxes and contributions from the concrete and shale are negligible. Moreover we observe that between 50 and 100 years, the volume of rejected gas is doubled. On the other hand, it is multiplied by less than 5 between 100 and 500 years. This is explained by the decrease of CO_2 fluxes linked to the increase in water saturation of the backfill material linked to the hydration from the shale, hence decreasing gas permeability (Fig. 7).

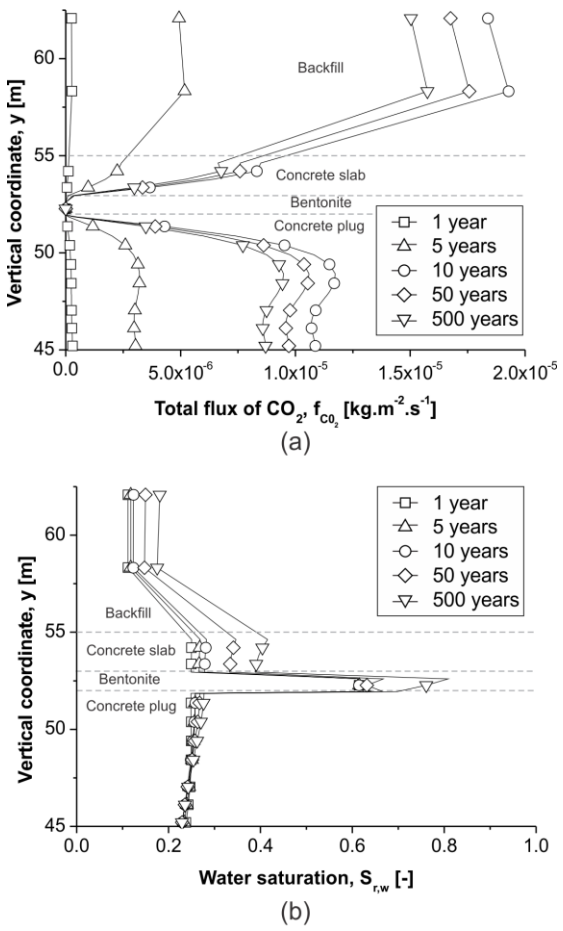

Fig. 7: Evolution of total gas flux and water saturation along the shaft axis during CO_2 storage in the coal mine

Time	Backfill	Concrete support	Shale
1 year	65 kg	-	-
5 years	1,01 10^4 kg	0,68 kg	-
10 years	5,68 10^4 kg	5,45 kg	0,78 kg
20 years	1,48 10^5 kg	13,82 kg	1,05 kg
50 years	4,04 10^5 kg	31,84 kg	1,66 kg
100 years	8,09 10^5 kg	53,39 kg	2,63 kg
500 years	3,87 10^6 kg	150,34 kg	9,64 kg

Table 3: Contribution of the different materials to the total mass of CO_2 rejected to the atmosphere, determined at 50 meters depth

Finally, hydromechanical couplings appear to be relatively weak and CO_2 injection hardly modifies the stress state in the host rock. This is partly due to the relatively small gas pressures involved in the problem, and partly due to the constitutive models used.

6.3. Sensitivity analysis

In the previous modelling some characteristics or parameters of the host rock and concrete were assumed due to the lack of experimental data. In this section, a sensitivity analysis is carried out in order to assess the influence of these parameters on the overall performance of the system.

6.3.1. Host rock initial degree of saturation

As the initial degree of saturation of the host rock is initially unknown, it seems particularly pertinent to analyse its influence. All other parameters kept constant, the initial degree of saturation of the host rock appears to have limited influence on the total mass of rejected CO_2 and the volume of gas that is rejected through the host rock increases slightly (Fig. 8). Indeed, changes in the host rock initial degree of saturation do not modify significantly the release mechanisms and concrete remains the main vector for CO_2 release.

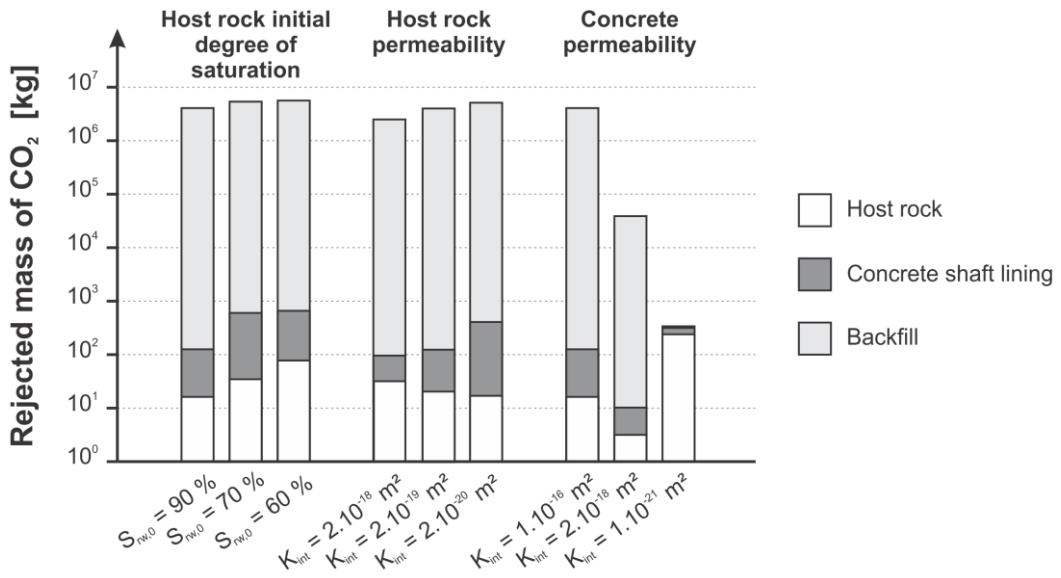

Fig. 8: Contribution of the different materials to the total mass of CO_2 rejected to the atmosphere, determined at 50 meters depth after 500 years. Rejected mass of CO_2 is expressed on a logarithmic scale

6.3.2. Host rock permeability

The host rock permeability has relatively little influence on the overall performance of the system, all other parameters kept to their reference values (Fig. 8). Still, we observe that the rejected mass of CO_2 tends to increase when the host rock permeability decreases. A decrease of the rock permeability enhances the contribution of the concrete shaft lining to the release of carbon dioxide to the atmosphere. Indeed, in this case, the lower permeability of the host rock limits water flow from the shale to the sealing system which in turn results in a lower degree of saturation of the sealing materials (Fig. 9), hence higher gas permeability.

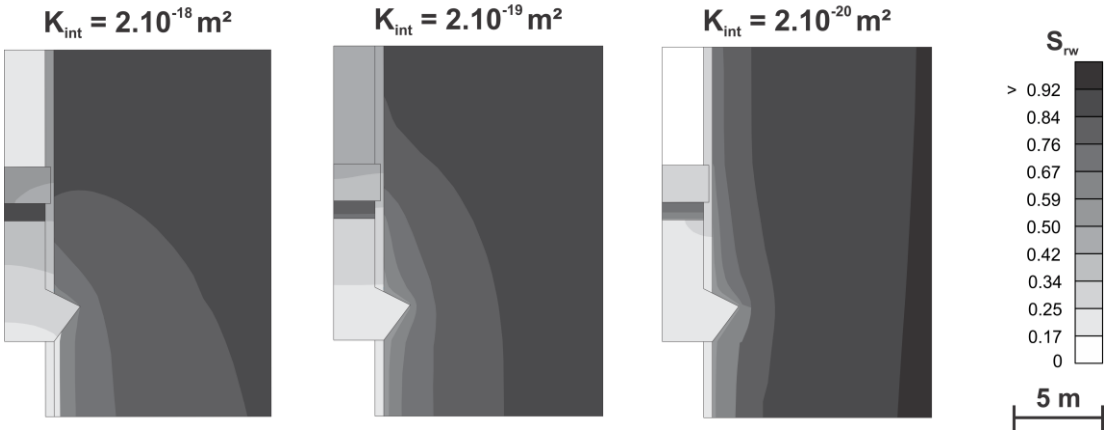

Fig. 9: Distribution of water degree of saturation after 500 years

6.3.3. Concrete permeability and time-dependent behaviour

In the context of CO_2 injection, the hydromechanical properties of concrete will evolve, especially as a consequence of cement carbonation (Takla et al. 2011, Zhang and Bachu 2011). Cement carbonation results from the instability of portlandite and calcium silicate hydrate (CSH) phases under the influence of CO_2. The carbonation of portlandite leads to the formation

of calcite, while the carbonation of the CSH is associated to the formation of calcite and silica gel. Cement carbonation comes generally along with a decrease in porosity (as a result of the increase of the solid phases) and a decrease in permeability. It has therefore positive effects regarding gas transfer (Takla et al. 2011). Cement carbonation has also positive effects on the mechanical properties of the material, as evidenced by Takla et al. (2011). Advanced constitutive models were proposed by Fabbri et al. (2012) and Vallin et al. (2013) to account for cement carbonation.

In the present study, the effects of CO_2 on the hydromechanical behaviour of concrete are not taken into account. Instead, a sensitivity analysis on concrete permeability is performed. Fig. 8 presents the contribution of the host rock, the concrete shaft lining and the backfill to the release of CO_2, for different values of concrete permeability. Interestingly, it is observed that the mass of CO_2 rejected trough the backfill is proportional to the concrete intrinsic permeability. However, the concrete permeability changes also the gas leakage process. Given its intrinsic permeability and degree of saturation, the host rock has a permeability to gas of the order of 10^{-22} m². Now, in the reference case ($K_{int,concrete}$ = 10^{-16} m²), the gas permeability of concrete is of the order of 10^{-17} m² and CO_2 preferentially flows through the concrete elements, and then the backfill. When the intrinsic permeability of concrete is decreased up to 2.10^{-18} m², the permeability to gas of concrete is also decreased, but it remains higher than the one of the host rock. Consequently, concrete remains the main vector to gas flow, but the total rejected mass of CO_2 is decreased. However, when the intrinsic permeability of concrete is decreased up to 10^{-21} m², the permeability to gas of concrete becomes of the same order of magnitude to the one of the shale. In this case, the overall rejected mass of CO_2 is decreased, but the contribution of the host rock is more important as CO_2 fluxes are integrated over a larger domain. This explains the non-monotonous contribution of the host rock to CO_2 leakage.

7. Numerical modelling using interface finite elements

In the previous sections, perfect contact between the materials was assumed and gas leakage mechanisms were analysed assuming multiphase flow in the porous materials. The possibility of gas flow through the concrete lining/host rock interfaces (Fig. 1) is now considered. These interfaces are explicitly modelled using interface finite elements presented in the next section. The constitutive models and parameters adopted for the different materials are similar to those defined in the previous sections. As the study focuses on CO_2 leakage, only results from the last stage of the modelling are presented in the paper.

7.1. Interface finite elements

The zero-thickness coupled finite interface element presented in Cerfontaine et al. (2015) is extended to multiphase conditions. In order to describe fluid flow not only through the interface, but also within the interface, a three-node formulation is adopted (Fig. 10) and flow of water and gas is described in both longitudinal and transversal directions.

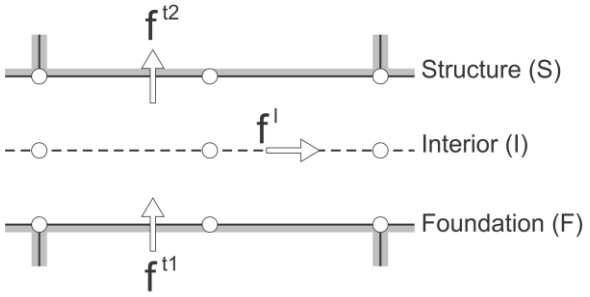

Fig. 10: Hydromechanical interface finite element

Transversal fluxes of water and CO_2 are written between both sides of the interfaces (called foundation and structure). They are expressed in the form:

$$f_w^{t1} = T_t \, t_{rw} \, (p_w^F - p_w^l) \, \rho_w \tag{16}$$

$$f_w^{t2} = T_t \, t_{rw} \, (p_w^l - p_w^S) \, \rho_w \tag{17}$$

$$f_{CO_2}^{t1} = T_t \, t_{rg} \, \left(p_g^F - p_g^l\right) \rho_{CO_2}$$

(18)

$$f_{CO_2}^{t2} = T_t \, t_{rg} \left(p_g^I - p_g^S\right) \rho_{CO_2}$$

(19)

where T_t is the transversal transmissivity and t_{rw} and t_{rg} are the water and gas relative transmissivities (accounting for partial saturation of the interfaces). The water pressures p_w^F, p_w^I and p_w^S, and gas pressures p_g^F, p_g^I and p_g^S correspond to pressures on the foundation, inside and structure side of the interface respectively.

Longitudinal fluxes of water and CO_2 account for advective and diffusive flows, and equations (4) to (7) are used to describe the flow within the interface. Advective fluxes of water and gas are computed using a generalized Darcy's law for unsaturated media:

$$q_w^l = -\frac{K_l \, k_{rll}}{\mu_w} \left(\underline{grad}(p_w) + g \, \rho_w \underline{grad}(y)\right)$$

(20)

$$q_g^l = -\frac{K_l \, k_{rlg}}{\mu_g} \left(\underline{grad}(p_g) + g \, \rho_g \underline{grad}(y)\right)$$

(21)

where K_l is the longitudinal intrinsic permeability and k_{rll} and k_{rlg} are the water and gas longitudinal relative permeabilities. Diffusion fluxes inside the fluid phases are calculated by means of Fick's law as in equations (10) and (11).

Finally, the mechanical behaviour of the interface is defined by the relationship between stress variation and variation of the relative displacement of both sides of the interface. The contact constraint is regularised by a penalty method and discretised on a segment-to-segment basis (Wriggers, 2006).

7.2. Interface properties

The properties of unsaturated interfaces are difficult to assess. Indeed, their estimation generally requires dedicated laboratory tests which are not available in the present study. Therefore, the water retention curve and relative permeability curves previously adopted for concrete are used to model the hydraulic behaviour of the interface, and the influence of the longitudinal permeability and the transversal transmissivity on the gas migration mechanisms is analysed.

Four scenarios are defined as limiting cases according to Table 4. Scenarios A and C consider a null longitudinal permeability and respectively low and high transversal transmissivities. These two first modelling allow assessing the impact of transversal flow on the CO_2 migration process. The effect of the longitudinal permeability is investigated in scenarios B and D, for which a longitudinal permeability of 5.10^{-8} m² is adopted. According to the definition of these four scenarios, it should be noted that scenario C is similar to the reference case defined in section 4. Indeed, the absence of longitudinal permeability does not lead to preferential pathways for gas migration, and the important transversal transmissivity tends to perfect contact conditions.

	No longitudinal permeability $K_l = 0\ m^2$	High longitudinal permeability $K_l = 5.10^{-8}\ m^2$
Low transversal transmissivity $T_t = 10^{-15}\ m.Pa^{-1}s^{-1}$	A	B
High transversal transmissivity $T_t = 10^{-3}\ m.Pa^{-1}s^{-1}$	C	D

Table 4: Longitudinal permeabilities and transversal transmissivities used in the four scenarios

7.3. Model results and analysis

Fig. 11 presents the distributions of gas pressure around the shaft sealing system for the four scenarios defined in Table 4. The gas pressure distribution for scenario C is close to the one observed in the absence of interface and will therefore be used as a reference for the analysis of

the other three scenarios. Now, let us consider a decrease in the transversal transmissivity (scenario A). This situation corresponds for instance to the presence of soft and low-permeability clay layer formed by the weathering of the shale rock. In this case, the lining/host rock interface acts as a low permeability layer reducing the diffusion of gas pressure into the shale rock. Imperfect contact between the concrete lining and the host rock could also occur without impervious filling. In this case, the longitudinal permeability of the interface is higher (scenarios B and D) and the interface acts as a preferential pathway for gas migration. In scenarios B and D, the diffusion of gas pressures in the shale is reduced because the interface drains gas fluxes. The increase in gas pressures is however more important in scenario B for which the low transversal transmissivity of the interface limits gas flow to the interior of the interface.

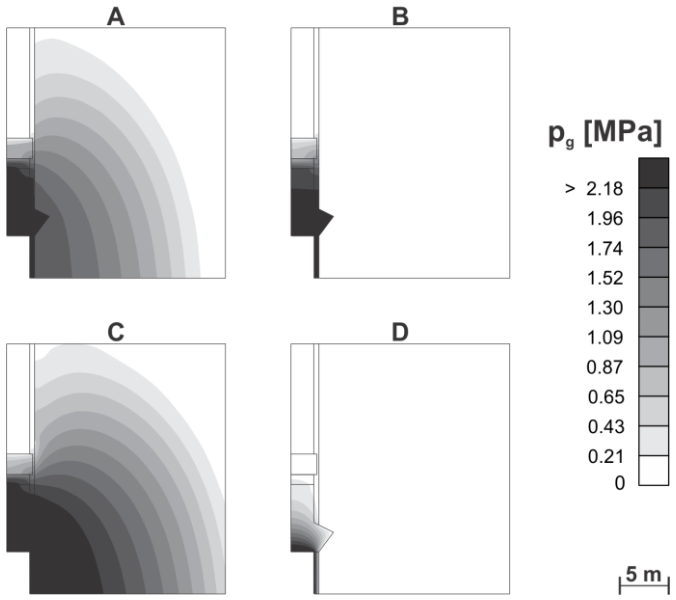

Fig. 11: Distribution of gas pressures in the different materials after 500 years. Influence of the longitudinal permeability and transversal transmissivity of the host rock / concrete lining interface

8. Conclusions

This paper has examined the problem of shaft sealing in relation to the use of abandoned coal mines as reservoirs for CO_2 sequestration. Basically the objective of the modelling was to achieve a better understanding of the CO_2 transfer mechanisms through and around a shaft and its sealing system. In addition, the study aimed at assessing the potential impacts of interfaces between the concrete lining and the host rock on CO_2 leakage mechanisms. The abandoned coal mine of Anderlues, which was used for seasonal storage of natural gas, has been considered for the study. Particular attention has been paid to the selection of realistic values for the model parameters. Experimental data on Westphalian shale from Beringen mine (Ramos da Silva et al., 2008) have been used while properties from materials studied for the underground disposal of nuclear waste have been adopted for the sealing system.

In order to establish realistic hydromechanical conditions prior CO_2 injection, shaft excavation and ventilation have been reproduced. The efficiency of the sealing system has then been evaluated simulating the injection of carbon dioxide in the coal mine. According to the analysis, CO_2 transfers occur mainly through the concrete elements. Moreover the bentonite buffer has shown limited efficiency as CO_2 bypasses it to flow though the concrete support. The design of the sealing system may therefore be the origin of inefficiency.

Furthermore the influence of interfaces between the concrete lining and the shale rock has been analysed by defining four limiting scenarios. From the analysis of these scenarios, it appears that the behaviour of interfaces is a critical issue regarding CO_2 leakage. Indeed, bad contact between the materials, possibly associated to poor filling of the interface, could lead to preferential pathways for CO_2 migration and jeopardize the viability of the storage site.

Acknowledgments

The authors gratefully acknowledge John-Henri Van Massenhove and Maxime Latinis from Fluxys for providing information on the Anderlues natural gas storage site.

References

Alonso J, Navarro V, Calvo B and Asensio (2012). Hydro-mechanical analysys of CO_2 storage in porous rocks using a critical state model. International Journal of Rock Mechanics & Mining Sciences 54: 19-26.

Bemer E, Longuemare P and Vincké O (2004) Poroelastic parameters of Meuse/Haute Marne argilites: effect of loading and saturation states. Applied clay Science 26: 359–366.

British Geological Survey, BGS (2008). An appraisal of underground gas storage technologies and incidents for the development of risk assessment methodology. BGS, Health and safety executive, Nottingham, UK: 350 p.

Boulvain F and Pingot J-L (2012). Genesis of Walloon underground [in French]. Classe des Sciences, Académie royale de Belgique:190 p.

Celia MA, Bachu S, Nordbotten JM, Gasda SE and Dahle HK (2005) Quantitative estimation of CO_2 leakage from geological storage: analytical models, numerical models, and data needs. In: Proceedings of the 7th International Conference on greenhouse Gas Control Technologies, Vancouver: 663–671.

Cerfontaine B, Dieudonne AC, Radu JP, Collin F and Charlier R (2015) Three-node zero-thickness hydro-mechanical interface finite element for geotechnical applications. In: Schrefler B, Oñate E and Papadrakakis M (Eds) VI International Conference on Computational Methods for Coupled Problems in Science and Engineering.

Charlier R, Radu J-P and Collin F (2001). Numerical modelling of coupled transient phenomena. Revue Française de Génie Civil 5(6): 719-741.

Chen W, Liu J, Brue F, Skoczylas F, Davy CA, Bourbon X and Talandier J. (2012) Water retention and gas relative permeability of two industrial concretes. Cement and Concrete Research 42: 1001-1013.

Chen Z, Liu J, Elsworth D, Connell L and Pan Z (2010). Impact of CO_2 injectiona and differential deformation on CO_2 injectivity under in-situ stress conditions. International Journal of Coal Geology 81: 97-108.

Collin F, Li XL, Radu J-P and Charlier, R (2002). Thermo-hydro-mechanical coupling in clay barriers. Engineering Geology 64: 179-193.

Connell LD (2009). Coupled flow and geomechanical processes during gas production from coal seams. International Journal of Coal Geology 79: 18-28.

Corey A.T., Kemper W.D. and Dane J.H. (2010). Revised model for molecular diffusion and advection. Vadoze Zone Journal 9(1): 85–94.

Cosenza P, Ghoreychi M, de Marsily G, Vasseur G and Violette S (2002) Theoretical prediction of poroelastic properties of argillaceous rocks from in situ specific storage coefficient. Water Resources Research 38(10): 25–1–25–12.

Delmer A, Dusar M and Delcambre B (2011). Upper Carboniferous lithostratigraphic units (Belgium). Geologica Belgica 4(1-2): 95-103.

Environmental Protection Agency, EPA (1998). Technical and economic assessment of coalbed methane storage in abandoned mine workings. EPA, Coalbed methane outreach program, Atmospheric pollution prevention division, Washington d.C., USA: 48 p.

Espinoza DN, Vandamme M, Pereira JM, Dangla P and Vidal-Gilbert S (2014). Measurement and modelling of adsorptive poromechanical properties of bituminous coal cores exposed do CO2: Adsorption, swelling strains, swelling stresses and impact on fracture permeability. International Journal of Coal Geology 134–135, 80–95.

Fabbri A, Jaquemet N and Seyedi DM (2012) A chemo-poromechanical model of oilwell cement carbonation under CO_2 geological storage conditions. Cement and Concrete Research 42(1): 8–19.

Fluxys (1990). Modification of the shaft n°2 in Anderlues [in French]. Technical note: 49 p.

Gaucher EC, Defossez PDC, Bizi M, Bonijoly D, Disnar JR, Laggoun-Défarge F, Garnier C, Finqueneisel G, Zimny T, Grgic D, Pokryszka Z, Lafortune S and Vidal Gilbert S (2011). Coal laboratory characterisation for CO2 geological storage. Energy Procedia 4: 3147-3154.

Gerard P, Charlier R, Barnichon J-D et al. (2008). Numerical modelling of coupled mechanics and gas transfer around radioactive waste in long-term storage. Journal of Theoretical and Applied Mechanic 8(1-2): 24-44.

Gerard P, Charlier R, Chambon R and Collin F (2008). Influence of evaporation and seepage on the convergence of a ventilated cavity. Water Resources Research 44(5), doi:10.1029/2007WR006500.

Ghiste S (1990). Geotechnical Map 46.7.5 to 8 Charleroi. Fontaine-l'Eveque – Marchienne au Pont. Imprimerie du Ministère des Travaux Publics. 9 maps: 52 p.

Gray I (1987). Reservoir engineering in coal seams: part 1 – the physical process of gas storage and movement in coal seams. SPE 12514. SPE Reservoir Engineering: 28-34.

Hou MZ, Zhou L and Luo X (2010) THM:C Coupled models for borehole stability in tight gas sandstone and shale formations. In: Hou MZ, Xie H and Yoon J (Eds) Underground storage of CO2 and Energy: 345–352.

Houtrelle S (1999). Natural gas storage in abandoned coal mine. Geological approach to the site of Anderlues (in French). Master thesis, Faculté Polytechnique de Mons, 50 p.

Jalili P, Saydam S and Cinar Y (2011). CO_2 storage in abandoned coal mines. In: Proceedings, 2011 Underground coal operator's conference, Wollongong, University of Wollongong: 335-360.

Kempka T, Waschbüsch M, Fernandez-Steeger TM and Azzam R (2006). Sorptive storage of CO_2 on coal dust and flotation waste from coal processing in abandoned coal mines. In: van Cotthem A, Charlier R, Thimus J-F, Tshibangu J-P (Eds) EUROK 2006 – Multiphysics Coupling in Long Term Behaviour in Rock Mechanics, Liege: 67-74.

Laloui L and Li C (2015). Carbon dioxide injection into deep aquifers: a geomechanical perspective. In: Oka, Murakami, Uzuoka and Kimoto (Eds) Computer Methods and Recent Advances in Geomechanics: 45–50.

Lutynski M (2010). A concept of enhanced methane recovery by high pressure CO_2 storage in abandoned coal mine. Gospodarka Surowcami Mineralnymi 26(1): 93-104.

Nuth M and Laloui L (2007). Effective stress concept in unsaturated soils: clarification and validation of a unified framework. International Journal for Numerical and Analytical Methods in Geomechanics 32: 771 – 801.

Piessens K and Dusar M (2004) Feasibility of CO_2 sequestration in abandoned coal mines in Belgium. Geologica Belgica 7(3-4): 165–180.

Piessens K, Laenen B, Nijs W, Mathieu P, Baele JM, Hendriks C, Bertrand E, Bierkens J, Brandsma R, Broothaers M, de Visser E, Dreesen R, Hildenbrand S, Lagrou D, Vandeginste V and Welkenhuysen K (2008) Policy Support System for Carbon Capture and Storage "PSS–CCS". Final report (phase I). 269p.

Pini R, Ottiger S, Burlini L, Storti G and Mazzotti M (2009). CO_2 storage through ECBM recovery: an experimental and modelling study. Energy Procedia 1: 1711-1717.

Pintado X, Ledesma A and Lloret A. (2002) Backanalysis of thermohydraulic bentonite properties from laboratory tests. Engineering Geology 64: 91-115.

Pollock DW (1986). Simulation of fluid flow and energy transport processes associated with high-level radioactive waste disposal in unsaturated alluvium. Water Resources Research 22: 765-775.

Ramos da Silva M, Schroeder C and Verbrugge J-C (2008). Unsaturated rock mechanics applied to a low-porosity shale. Engineering Geology 97(1-2): 42-52.

Romanov VN, Ackman TE, Soong Y and Kleinman RL (2009). CO_2 storage in shallow underground and surface coal mines: challenges and opportunities. Environmental Science and Technology 43(3): 561-564.

Rutqvist J and Tsang CF (2002). A study of caprock hydromechanical changes associated with CO_2-injection into a brine formation. Environmental Geology 42(2-3): 296-305.

Seidle JP and Huitt IG (1995). Experimental measurement of coal matrix shrinkage due to gas desorption and implications for cleat permeability increases. SPE 30010, International Meeting on Petroleum Engineering, Beijing, China.

Schultz K (1998). Gas storage at the abandoned Leyden coal mine near Denver, Colorado. EPA-report, contract 68-W5-0018, prepared by Raven Ridge Resources Inc.: 12 p.

Shi JQ and Durucan S (2009). A coupled reservoir-geomechanical simulation study of CO2 storage in a nearly depleted natural gas reservoir. Energy Prcedia 1: 3039-3046.

Sy S, Fabbri A, Gravaud I and Seyedi D (2012) Evaluation of the CO_2 leakage risk along the abandoned wells in the French context. Energy Procedia 23: 480–486.

Vallin V, Pereira JM, Fabbri A and Wong H (2013) Numerical modelling of the hydro-chemo-mechanical behaviour of geomaterials in the context of CO_2 injection. International Journal for Numerical and Analytical Methods in Geomechanics 37(17): 3052–3069.

Vandeloise R (1969). Firedamp capture from the old works of the Anderlues colliery [in French]. Institut National des Industries Extractives, Technical bulletin "Mines and quarries" 119: 35 p.

Van Genuchten MT (1980). A closed-form equation for predicting the hydraulic conductivity of unsaturated soils. Soil Science Society of America Journal 44: 492:498.

Van Tongeren P and Dreesen R (2004). Residual space volumes in abandoned coal mines of the Belgian Campine Basin and possibilities for use. Geologica Belgica 7(3-4):157-164.

Vidal-Gilbert S, Nauroy JF and Brosse E (2009). 3D geomechanical modelling for CO2 geologic storage in the Dogger carbonates of the Paris Basin. International Journal of Greenhouse Gas Control 3: 288-299.

Vilarrasa V, Bolster D, Olivella S and Carrera J (2010). Coupled hydromechanical modelling of CO2 sequestration in deep saline aquifers. International Journal of Greenhouse Gas Control 4(6): 910-919.

Watson T and Bachu S (2009) Evaluation of the potential for gas and CO2 leakage along wellbores. SPE Drilling & Completion 24(1): 115–126.

White CM, Smith DH, Jones KL, Goodman AL, Jikich SA, La Count RB, Du Bose SB, Ozdemir E, Morsi BI and Schroeder KT (2005). Sequestration of carbon dioxide in coal with enhanced coalbed methane recovery – a review. Energy & Fuels 19(3): 659-724.

Wileveau Y (2005) THM behaviour of host rock (HE-D) experiment: Progress report Part 1: Technical report TR2005-03. Mont Terri Project.

Wriggers P (2006) Computational contact mechanics. Springer.